IHJPAS. 36 (4) 2023

Ibn Al-Haitham Journal for Pure and Applied Sciences
Journal homepage: jih.uobaghdad.edu.iq

Anticancer and Antioxidant activity of Gold Nanoparticles Biosynthesized Using *Acinetobacter baumannii*

Intesar H. Al-Abdeli*
Department of Biology, College of Education for Pure Sciences Ibn-Al-Haitham University of Baghdad, Baghdad, Iraq.

Esam J. Al-kalifawi
Department of Biology, College of Education for Pure Sciences Ibn-Al-Haitham University of Baghdad, Baghdad, Iraq.

***Corresponding Author:** Intessar.Hameed1102a@ihcoedu.uobaghdad.edu.iq

Article history: Received 13 December 2022, Accepted 20 Fabruary 2023, Published inOctober 2023.

doi.org/10.30526/36.4.3141

Abstract

In the current study, gold nanoparticles were made using Acinetobacter baumannii broth cultures. UV-visible spectroscopy, Fourier transform infrared spectroscopy (FT-IR), X-ray diffraction (XRD), transmission electron microscopy (TEM), field emission scanning electron microscopy (FE-SEM), atomic force microscopy (AFM), and zeta potential measurements were also used to study the properties of the Ab-AuNPs. The average size was 66 nm. The examination results proved that the Ab-AuNPs are semi-spherical and varied from 20 to 90 nm. MTT assays on the breast cancer cell line MCF-7 confirmed the anticancer activity in vitro. Cancer cells showed important cytotoxic activity for Ab-AuNPs. The mean lethal dose (IC_{50}) was 11.45 µg/mL, and the maximal inhibitory concentration was 25.50 mg/mL (63.00% and 86.33%, respectively), but ineffective against the normal cell line. MCF-10. The results proved that Ab-AuNPs have DPPH scavenging activity, which increases with increasing concentration of Ab-AuNPs, where the concentrations (3.1, 6.25, 12.5, 25, and 50) mg/ml gave DPPH scavenging activity with the following values: 37.87%, 50.13%, 59.33%, 75.55%, and 85.13%, respectively. The present study concludes that gold nanoparticles synthesized using *A. baumannii* broth cultures are easy to prepare, inexpensive, and non-toxic to normal cells. Meanwhile, they possess antioxidant and anticancer activity. So, it can be used as an alternative treatment.

Keywords: Gold nanoparticles, *Acinetobacter baumannii*, Antioxidant activity, Anticancer activities.

1. Introduction

Humans develop cancer, a potentially fatal condition, when normal cells are repeatedly exposed to carcinogens. Malignant tumors are collections of cancerous cells that differ from healthy cells in that they develop and spread uncontrollably [1]. Due to its inherent anticancer action, the field of study on using nanoparticles (NPs) to prevent tumor formation, growth, and progression is expanding. Physicochemical properties of NPs that contribute to their anticancer activity include either intrinsic characteristics, like the antioxidant effect, or processes dependent on external stimuli, like hyperthermia, in response to the application of infrared rays or magnetic fields. [2]. The capacity to enter and accumulate in cancer cells, followed by heat therapy. Then, the physical and chemical properties of the built-up gold nanoparticles can help kill cancer cells without hurting normal cells in the body. This is the goal of the treatment compared to other methods like chemotherapy, which has a lot of bad side effects for the patient, like hair loss and damage to healthy blood cells, causing vomiting or infections. [3].

Breast cancer is the second most common cancer diagnosis in women worldwide, and it is thought to be one of the main reasons that breast cancer accounts for 10.4% of all cancers in women. Men, however, frequently have the illness. [4]. The chances of having breast cancer have been found to increase with age. [5]. Due to their shape, size, excellent optical and electronic properties, high biocompatibility, and stability, gold nanoparticles are the most commonly used metal nanoparticles [6]. The biosynthesis of gold nanoparticles (AuNPs) would be easier if microorganisms, like bacteria and fungi, used methods that were clean, non-toxic, and good for the environment. Bacteria have always been the organisms of choice because they have the unique ability to make enzymes that are involved in the decrease and stability of metallic nanoparticles [7]. After gold nanoparticles enter most cancer cells, a series of processes evolve from the loss of mobile stability and an unstable oxidative state, and waves of free radicals begin to destroy and expand the nuclear envelope of the nucleus, and mitochondria unfold and increase the oxidative stress in the cell [8].

The current study aims to synthesize gold nanoparticles using *A. baumannii* broth culture and studies their antioxidant and anticancer activity**.**

2.Materials and Methods

2.1.Isolation and identification of *A. baumannii*

A. baumannii isolates were obtained from the microbiology laboratories at the Yarmouk Teaching Hospital. It was confirmed by Gram staining, the growth on different media, and biochemical tests, including catalase, coagulase, urease, and oxidase. Finally, the use of the Vitek 2 compact system [9].

2.2.Green synthesis of gold nanoparticles.

AuNPs were produced using the modified method described in [10]. Ten millilitres of stock solution of (HAuCl4.4H2O) were combined with (2,4,6,8 and10) mL of *A. baumannii* broth culture and heated at 50°C for 30 minutes on a magnetic hotplate stirrer. The resulting mixture [(HAuCl4.4H2O) +4mL of *A. baumannii* broth culture] was placed in a tube and subjected to a 30-minute ultrasonic bath. Following the development of red dots on the sides of the transparent tube inside the Ultrasonic Bath device, the colour of the solution changed from bright yellow to yellowish-orange. Each time the procedure is carried out, two ml of the bacterial broth culture is added to the gold salt solution while keeping the other parameters, such as the concentration of the gold salt solution, the temperature, the time, and a constant pH value, constant to produce an orange-coloured solution[(HAuCl4.4H2O) +6mL of *A. baumannii* broth culture]. It changed to a light purple[(HAuCl4.4H2O) +8mL of A. baumannii broth culture], then to a darker purple[(HAuCl4.4H2O) +10mL of *A. baumannii* broth culture], which showed that the gold nanoparticles in **Figure 1** had been created.

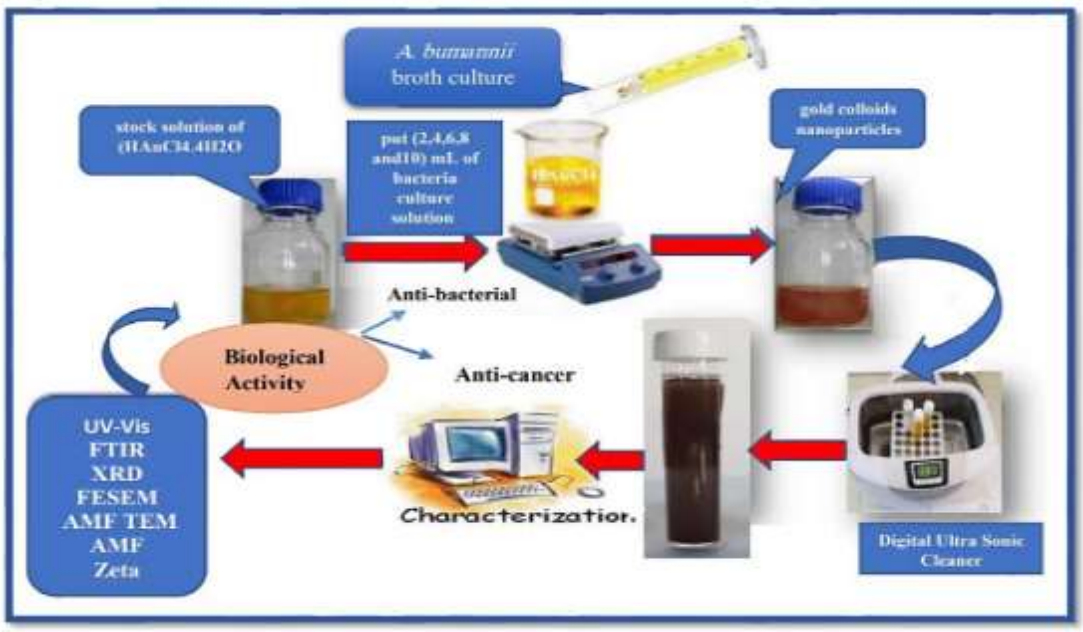

Figure 1. Illustration graphic of biosynthesis of gold nanoparticles using broth culture of *A. baumannii*.

2.3. Characterization of Gold Nanoparticles:

Ab-AuNPs were characterized using many techniques, including UV-Vis spectroscopy (Shimadzu UV-160A), FTIR spectroscopy (IRAffinity1Shmadzo), FE-SEM, TEM (Carl Zeiss, Germany), XRD (Philips PW1730), AMF, and Zeta potential measurement.

2.4. Biological applications of prepared gold nanoparticles

2.4.1.Cancer Cell Lines

The breast cancer cell line (MCF-7) was compared with the normal cell line (MCF-10) obtained from the cell bank of the Iraqi Center for Cancer and Medical Genetics Research. MCF-7 cells were maintained in RPMI-1640 supplemented with 10% fetal bovine serum, 100 units/mL of penicillin, and 100 µg/mL, of streptomycin. The cells were then passaged using trypsin-EDTA, reseeded at 80% confluence twice a week, and incubated at 37°C [11, 12].

2.4.2. Determination of cytotoxicity of Ab-AuNPs-using MTT assay

Using the MTT assay, the cytotoxic effect of Ab-AuNPs was measured according to [13]. For the MTT test, 96-well plates were used. 1×10^4cells/well cells/well were used to start the cell lines. After 24 hours or when a confluent.monolayer was formed different concentrations of the tested compounds were added to the cells. After 72 hours of treatment, the cell's ability to live was tested by taking out the medium, adding 28 µL of 2 mg/mL of 2 mg/mL, MTT, and letting them stay at 37 °C for 2.5 hours. After taking out the MTT solution, the crystals still in the wells were broken up by adding 130 L of DMSO (Dimethyl Sulphoxide) and shaking the wells for 15 minutes at 37 °C. The absorbency was measured at 575 nm with a microplate reader. The test was done three times. The following equation was used to determine how much cell growth was stopped (the percentage of cytotoxicity).

Inhibition rate = A- B/A*100"

A represents the optical density "of the standard, and B represents the optical density of the samples. To examine the shape of cells through an inverted microscope, the cells were seeded into 424-well micro-titration plates at a density of 1×105 cells mL−1 and incubated for 24 h at 37 °C. Then, cells were exposed to Ab-AuNPs.at IC50 for 24 hours. After the exposure time, the plates were stained with crystal violet and incubated at 37 °C for 10–15 minutes. The stain was gently washed away with tap water until the dye was eliminated. At 40×magnification, the cells were observed with an inverted microscope, and images were captured with a digital camera attached to the microscope.

2.4.3.Determination of DPPH Scavenging Assay of Ab-AuNPs

Free Radical Scavenging (DPPH) Activity Assay was used to test the antioxidant activity of the biosynthesized Ab-AuNPs. [14].

2.5. Statistical analysis

GraphPad.Prism 6 was used to analyze the data which was presented as the mean standard deviation±(SD) for three replicates per experiment. [15].

3.Results

Figure 2 shows the change in colour from yellow to dark violet, evidence of the biosynthesis of Ab-AuNPs using *A. baumannii* broth culture.

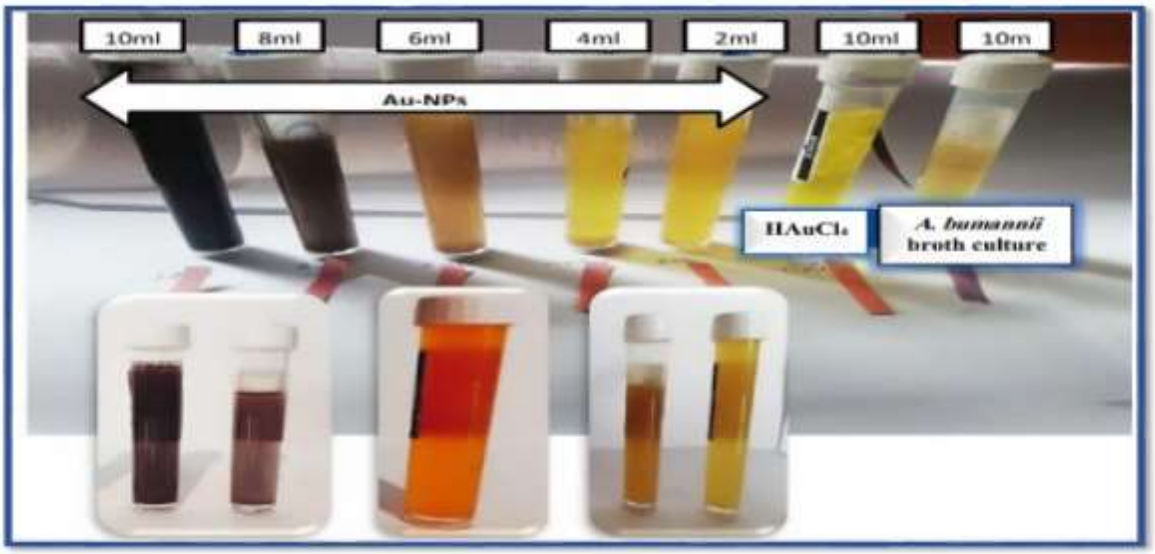

Figure 2. Exhibit solutions after changing their colour from yellow to dark violet.

3.1. UV-Visible analysis

Figure 3 shows the UV-Visible spectrum of Ab-AuNPs made with an *A. baumannii* broth culture. Ab-AuNPs had surface plasmon resonance (SPR) bands around 574 nm in their UV-Visible spectra While the absorbance peak of *A. baumannii* broth culture was at 301.5 nm by UV-Visible spectrophotometer.

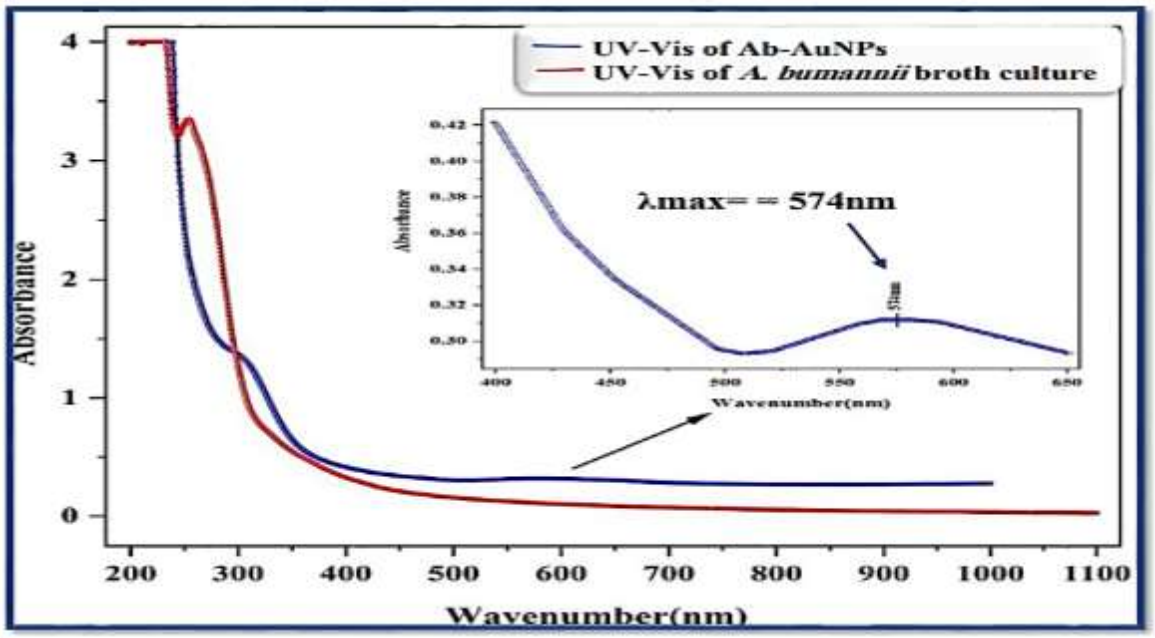

Figure 3. UV-Vis spectrum of Ab-AuNPs colloidal and *A. baumannii* broth culture.

FT-IR spectra of Ab-AuNPs in **Figure 4** indicate the primary peaks at (3321.42, 2823.79, 2144.84, and 1631.78) cm^{-1}. The large1peak at 3321.421cm^{-1} is relativity O–H2stretching vibration.of hydrogen-bonded alcohols, phenol, and N-H stretching of amines or amides, Alkanes, aldehydes, and corrosive carboxylic compounds all exhibit the C = H stretch independently at

2823.79 cm-^{1}, where C=O stretching vibrations are present at 1631.78 cm-^{1}. The vibration of the FT-IR spectrum of synthesized Ab-AuNPs illustrated a decrease in the peak intensities of the functional groups compared with the functional groups in *A. baumannii* broth culture. It is possible to observe the appearance and the disappearance of some bonds and that some of the absorbances have decreased due to their consumption as a capping agent during the synthesis process. The absence of these functional groups in the synthesized Ab-AuNPs indicates the formation of Ab-AuNPs. Identified sharp peaks in the range of (578.64–748.38) cm-^{1} refer to the vibration of Au-NPs. This result means that Ab-AuNPs were formed successfully [16].

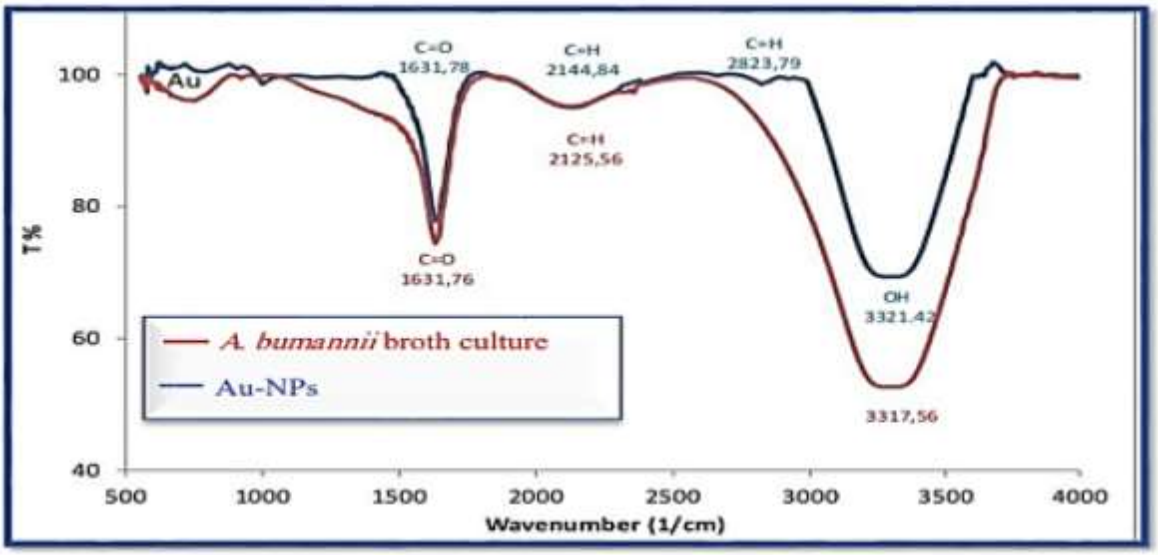

Figure 4. FT-IR spectrum of (read) *A. baumannii* broth culture and (blue) the Ab-AuNPs colloidal.

3.2.X-ray diffraction (XRD) analysis

Figure 5 displays the primary peaks at"111, 200, 220, and 311, which respectively, correspond to reflections with 2 values of the Bragg angles"38.18°, 44.51°, 64.80°, and 77.72°. These findings demonstrate that the tested substance is high-purity AuNPs. Using the.Debye-Scherrer, equation, the average crystallite size of the Ab-AuNPs in the arrangement was calculated to be 26.82 nm. [17].

Table 1. Structural parameter of Ab-AuNPs

Peak position(20°)	(hkl)	FWHM	Crystallite size (nm)	Average Crystallite D (nm)
38.18363	(111)	0.35431	23.72694466	26.82211084
44.51299	(200)	0.36896	23.26486114	
64.80844	(220)	0.38084	24.70709167	
77.72309	(311)	0.28667	35.58954589	

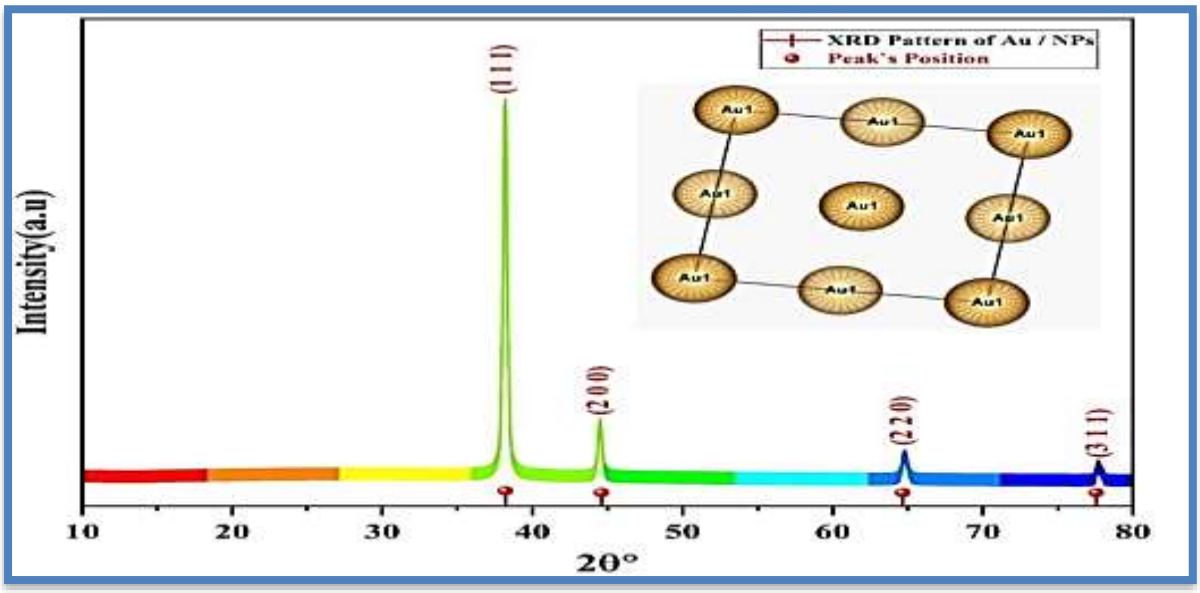

Figure 5. XRD of Ab-AuNPs biosynthesized using *A. baumannii* broth culture.

$D = K\lambda\beta COS\theta$

It elaborates on the connection between XRD peak broadening and crystallite size. Where D is the average size of nanoparticles, K is the Scherrer constant, which has a value of 0.9, Bragg's angle, and the wavelength of the X-ray radiation source, 0.15406 nm".

3.3. Transmission Electron Microscope (TEM) Examination

Ab-AuNPs had sizes that varied from 20 to 90 nm, with an average of 66 nm. **Figures 6, 7** demonstrate this. The reaction begins with the generation of semi-spherical Ab-AuNPs. Due to the high concentration of reducing factors in the *A. baumannii* broth culture, they subsequently cluster together along with rectangular, triangular, pentagonal, cylindrical, irregular, and polymorphic shapes.

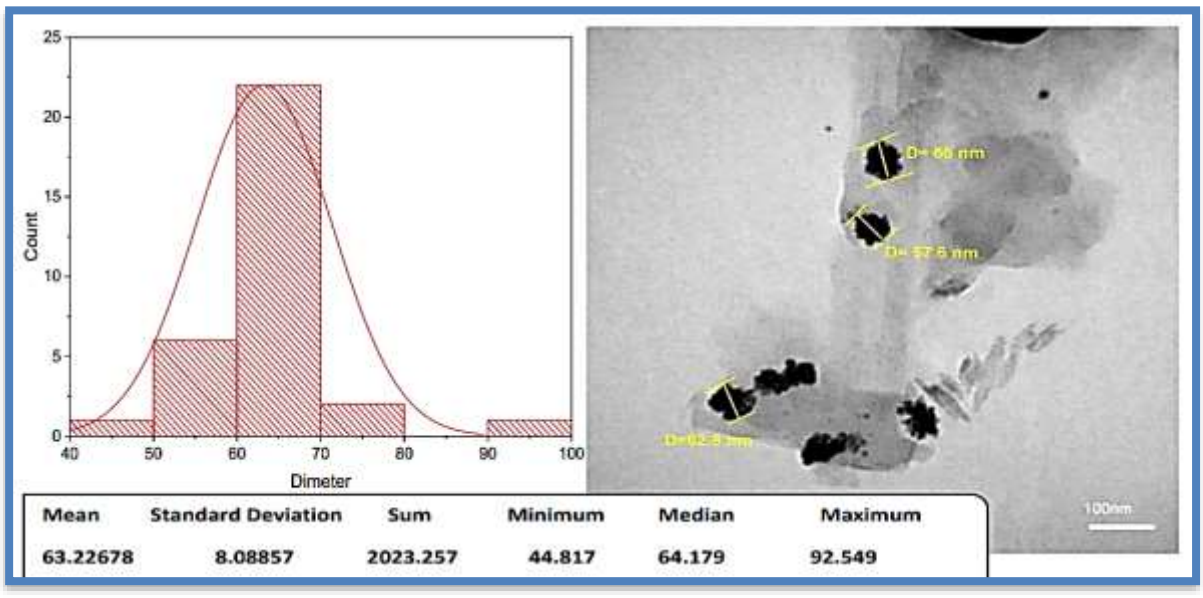

Figure 6. TEM image of diverse shapes of biosynthesized AuNPs using *A. baumannii* broth culture**.**

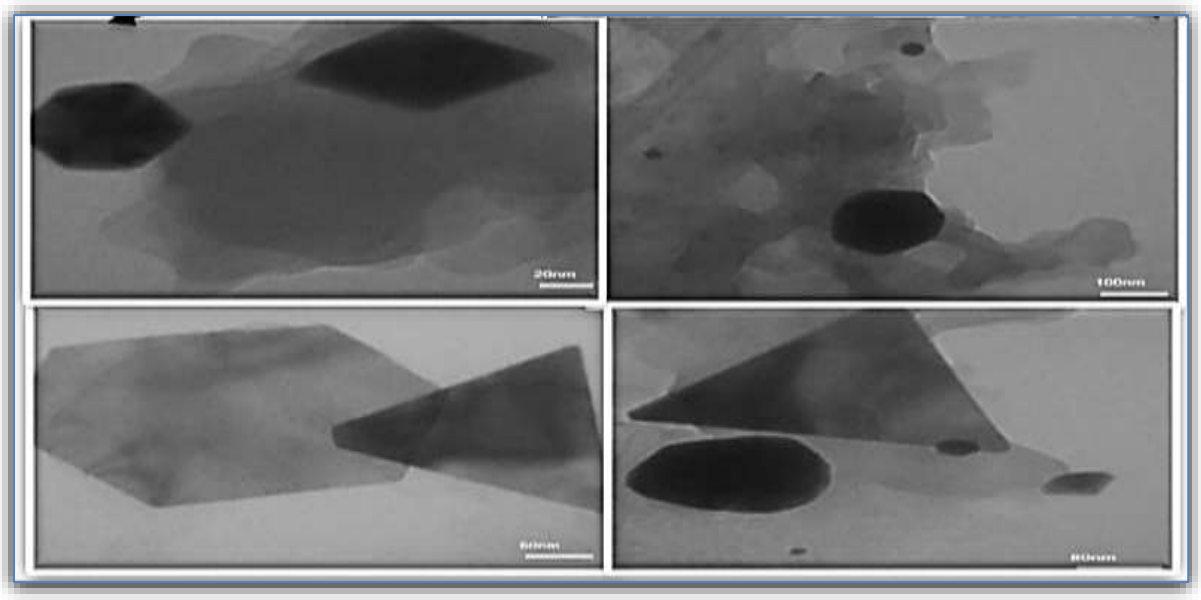

Figure 7. TEM image of biosynthesized Ab-AuNPs using *A. baumannii* broth culture, (a) Average diameters of gold nanoparticles, (b) diverse shapes.

3.4. Field Emission Scanning Electron Microscope analysis (FESEM)

As shown in **Figure 8**, the results show that Ab-AuNPs have a spherical form, a high degree of aggregation, and a size that ranges from (66-363) nm.

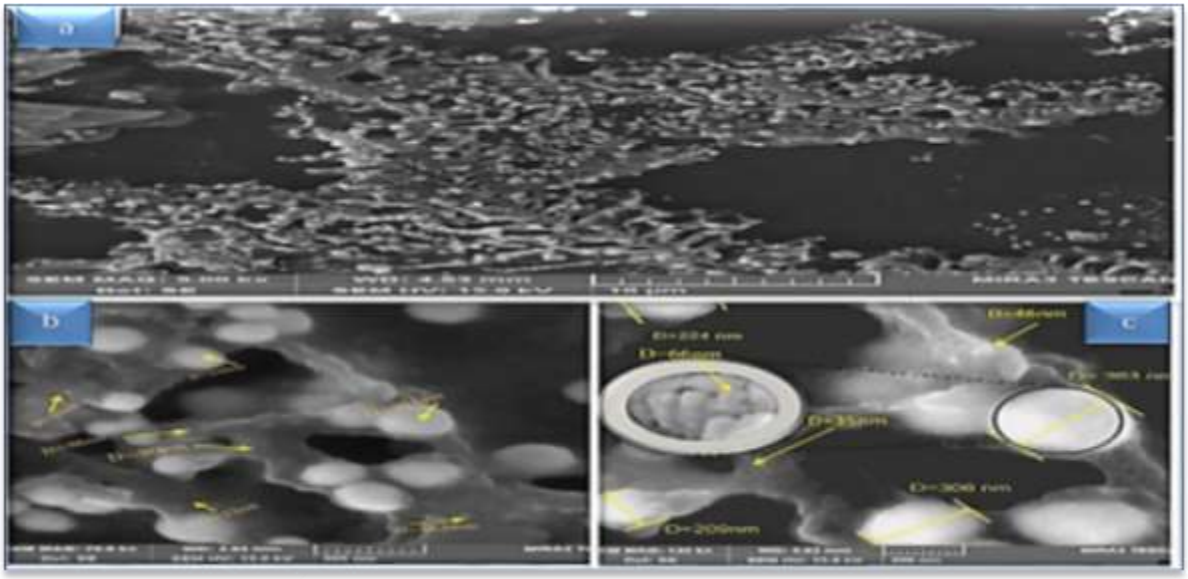

Figure 8. FESEM images of biosynthesized Ab-AuNPs using *A. baumannii* broth culture, a, b, c shows shapes of Ab-AuNPs.

3.5. AFM Analysis

The size distribution of Ab-AuNPs is seen in the 2D and 3D AFM pictures. No aggregation or agglomeration was observed in the slide sample of the AFM sample, which shows the great stability of the Ab-AuNPs produced after two months of AuNPs synthesis. The Ab- **Figure 9** shows that the size of the Ab-AuNPs particles ranged from 15 to 125 nm, with an average length of 63.82 nm.

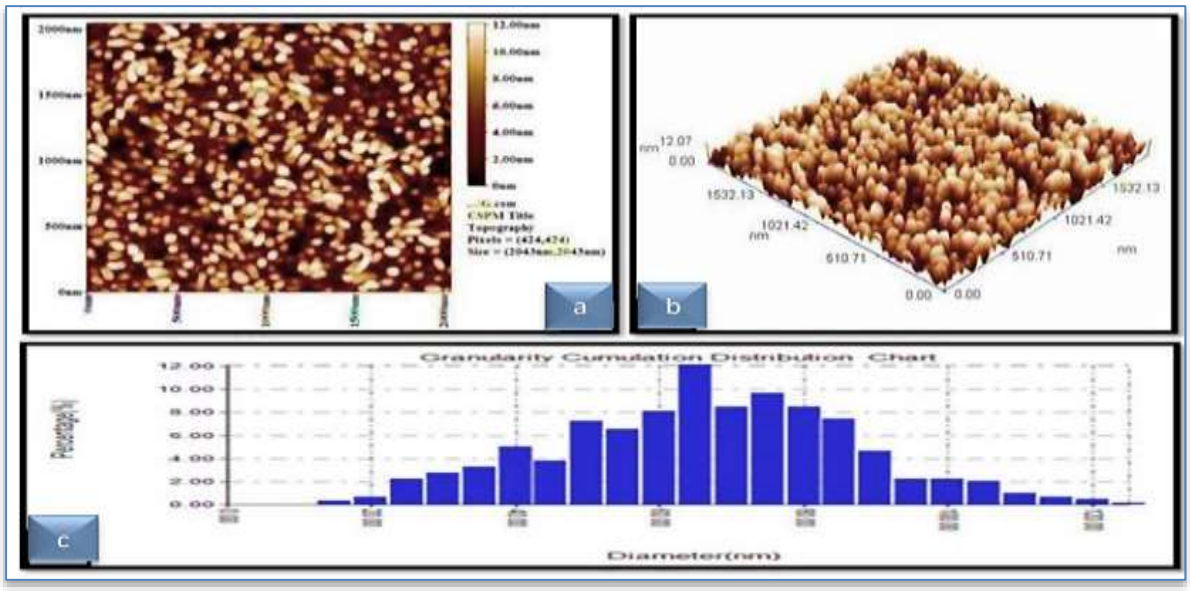

Figure 9. AFM images of biosynthesized Ab-AuNPs using *A. baumannii* broth culture, (a) Two-Dimensional, (b) Three-Dimensional, and (c) Average particle size.

3.6. Zeta Potential Measurements

Figure 10 shows that the biosynthesized Ab-AuNPs produced by *A. baumannii* broth culture had a Zeta Potential of -22 mV and less than 30 mV, indicating that the particles are stable and do not aggregate.

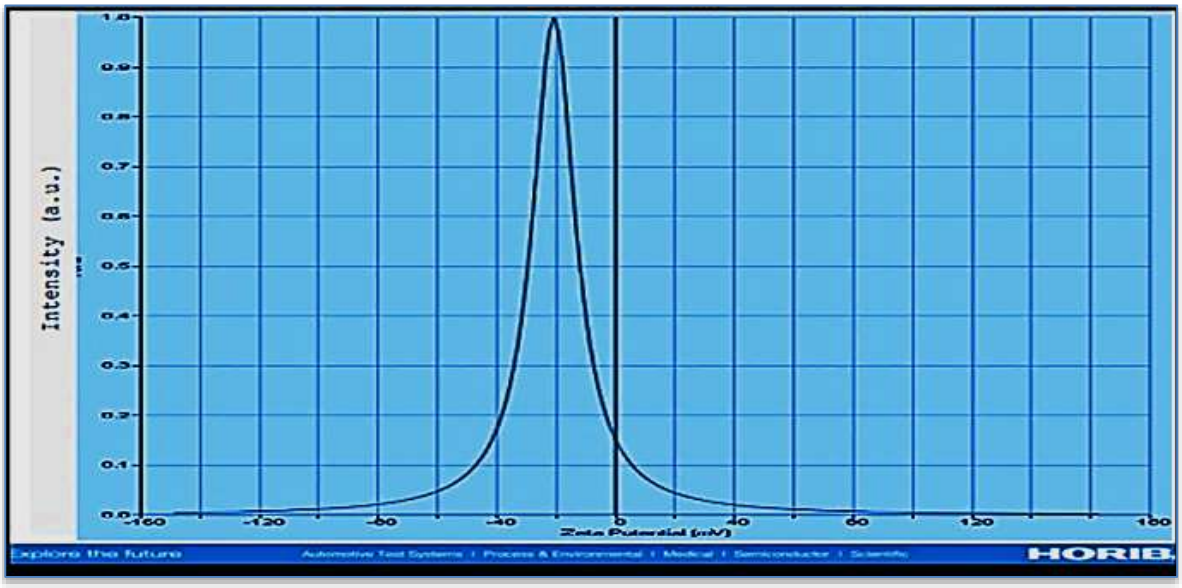

Figure 10. Zeta potential analysis of biosynthesized Ab-AuNPs using *A. baumannii* broth culture.

3.7. The Cytotoxic Effect of synthetic Ab-AuNPs

Figures 11, 12, 13 show that the cytotoxicity of the Ab-AuNPs was unaffected at 3.1 µg/ml, while the cytotoxicity increased significantly with increasing concentrations of Ab-AuNPs. Moreover, this assay showed that the minimum inhibitory concentration of MCF-7 cells was obtained by interaction with Ab-AuNPs at 6.25 mg/ml and 12.5 mg/ml, giving a reduction ratio (23.33% and 52.33%), respectively. However, the maximum concentration of inhibition was at 25

mg/ml and 50 mg/ml giving a reduction ratio (63.00% and 86.33%), respectively. This study showed a very important cytotoxic activity of Ab-AuNPs against the breast cancer cell line MCF-7 but ineffective against the normal cell line MCF-10 as shown in Figs. (15, 16). The results indicate the ability of Ab-AuNPs to suppress the growth of cell lines; this effect depends on the concentration. The median (IC50) was 11.45 mg/ml.

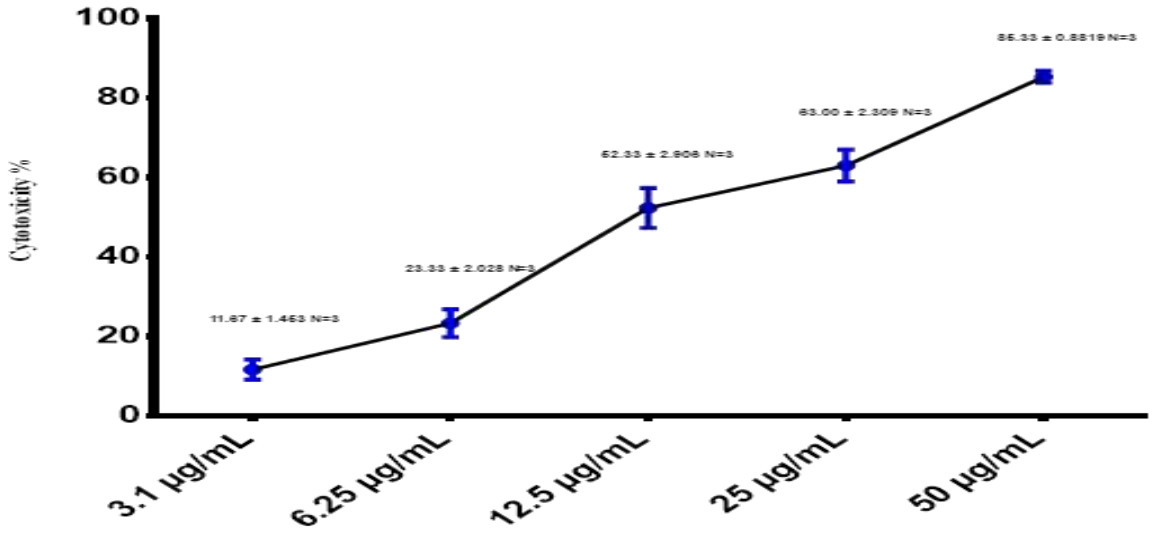

Figure 11. Cytotoxic effect of Ab-AuNPs in MCF-7 cells. IC50=11.45 µg/ml

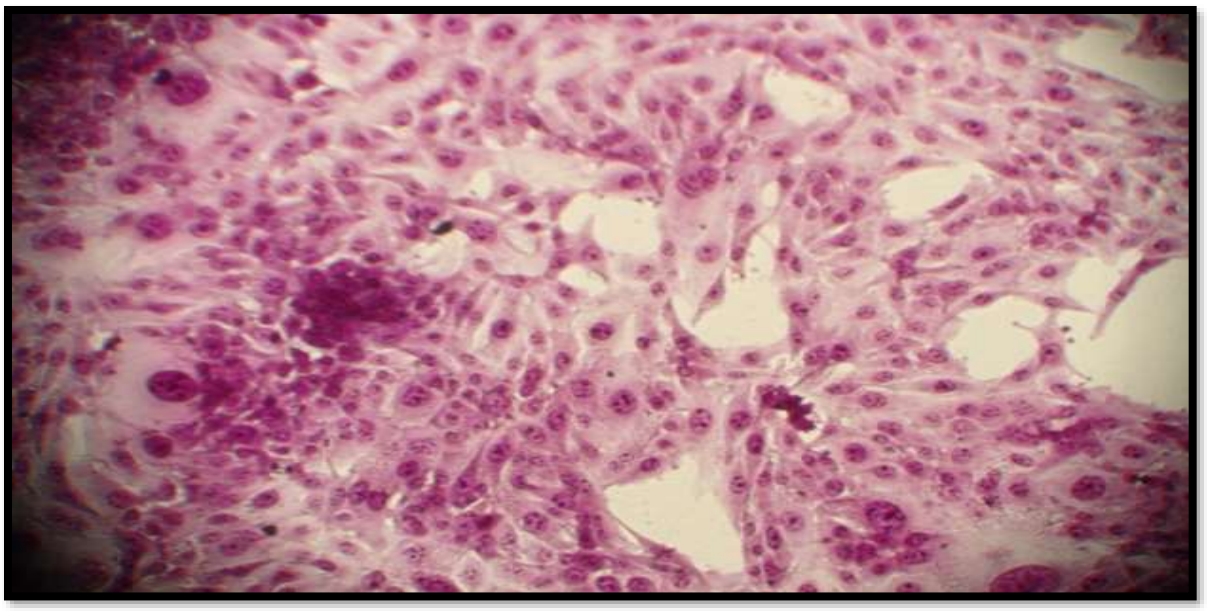

Figure 12. Control untreated MCF-7 cells

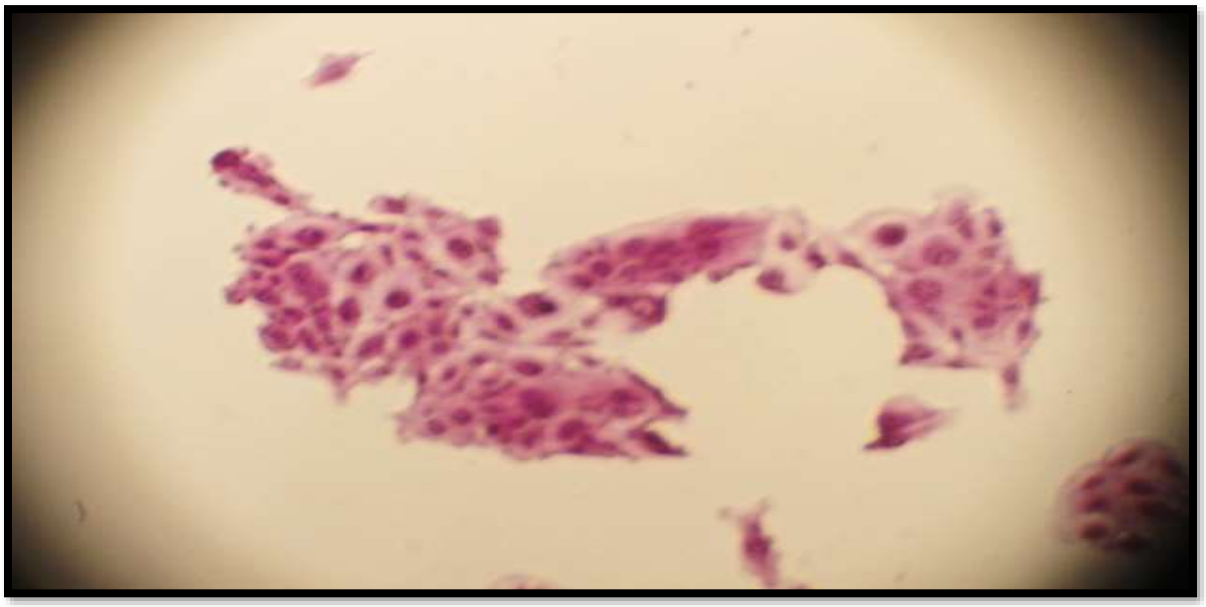

Figure 13. Morphological changes in MCF-7 cells after being treated with AuNPs

3.8. Cytotoxic Effect of synthetic Ab-AuNPs using *Acinetobacter bumannii solution* on MCF-10 normal cell lines:

Significant inhibition was demonstrated for the proliferation of the MCF-7 line opposite to the MCF-10 cells, the MCF-7 line, and the MCF-10 cells treated with Ab-AuNPs under the same time and conditions, "as shown in **Figure 14**.

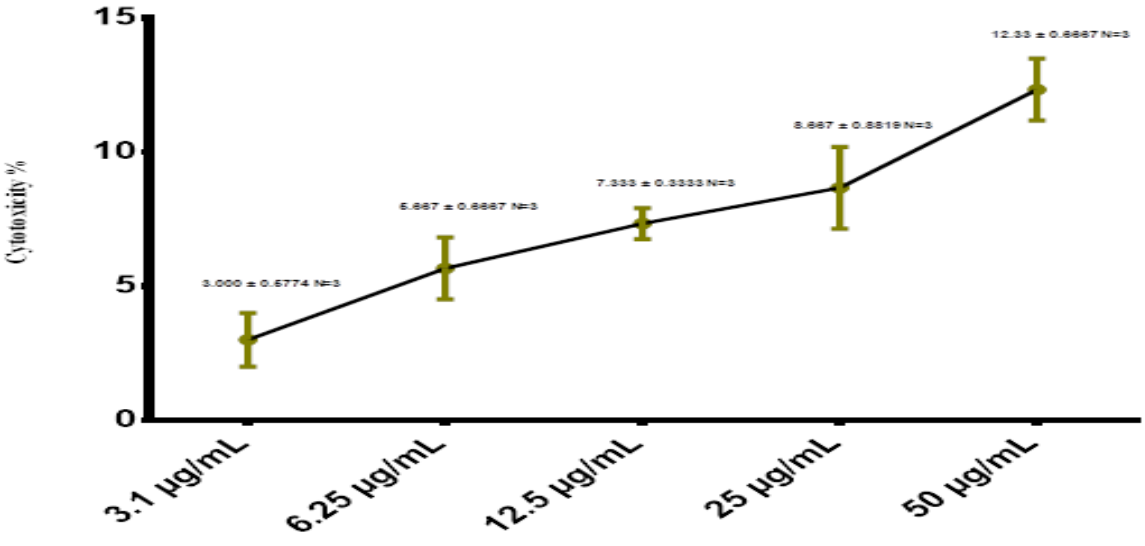

Figure 14. Cytotoxic effect of Ab-AuNPs in MCF-10 cells, IC50=11.45 µg/ml

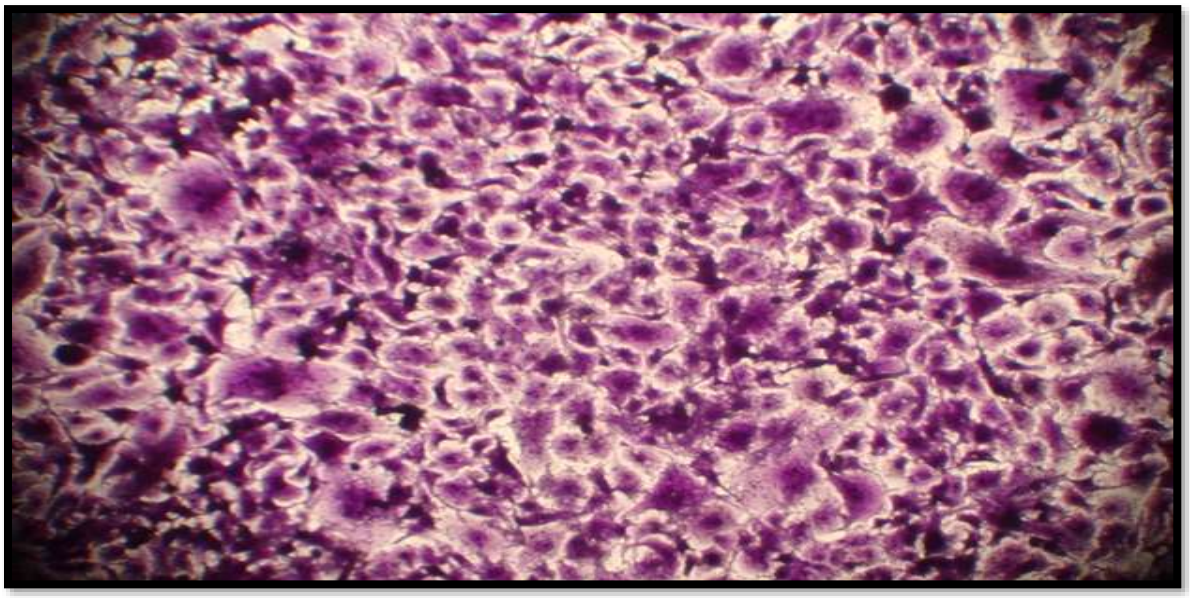

Figure 15. Control untreated MCF-10 cells.

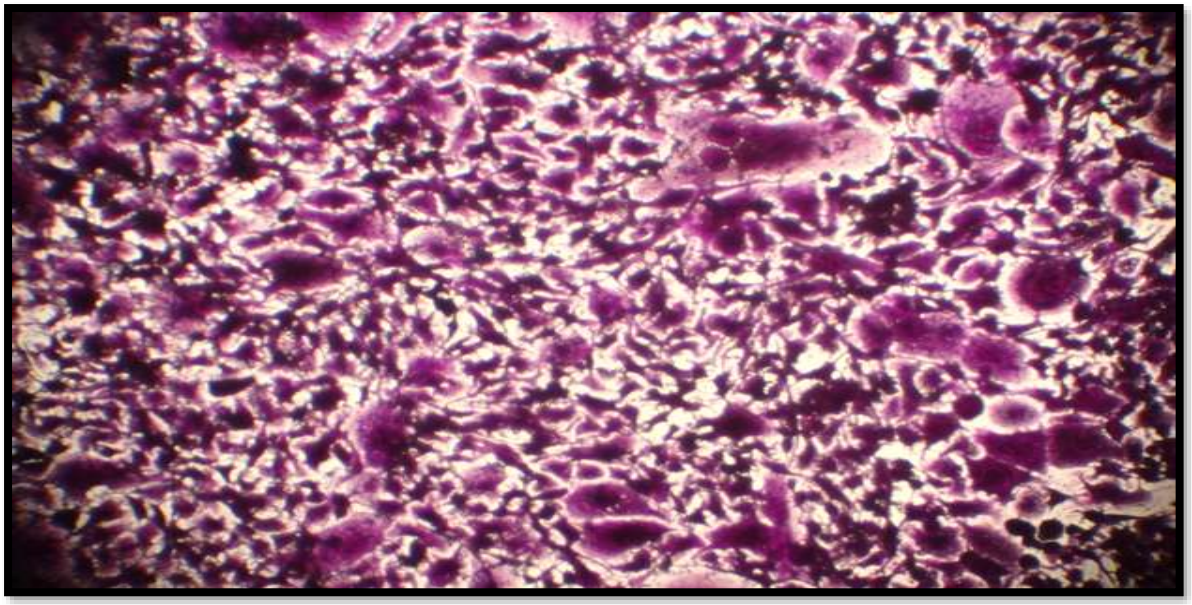

Figure 16. Morphological changes in MCF-10 cells after being treated with Ab-AuNPs

3.9. Antioxidant

3.9.1. DPPH Scavenging Assay

The results proved that Ab-AuNPs have DPPH scavenging activity, which increases with increasing concentrations of Ab-AuNPs. The concentrations (3.1, 6.25, 12.5, 25, and 50) mg/mL gave DPPH scavenging activity of 37.87%, 50.13%, 59.33%, 75.55%, and 85.13%, respectively, **Figure 17**.

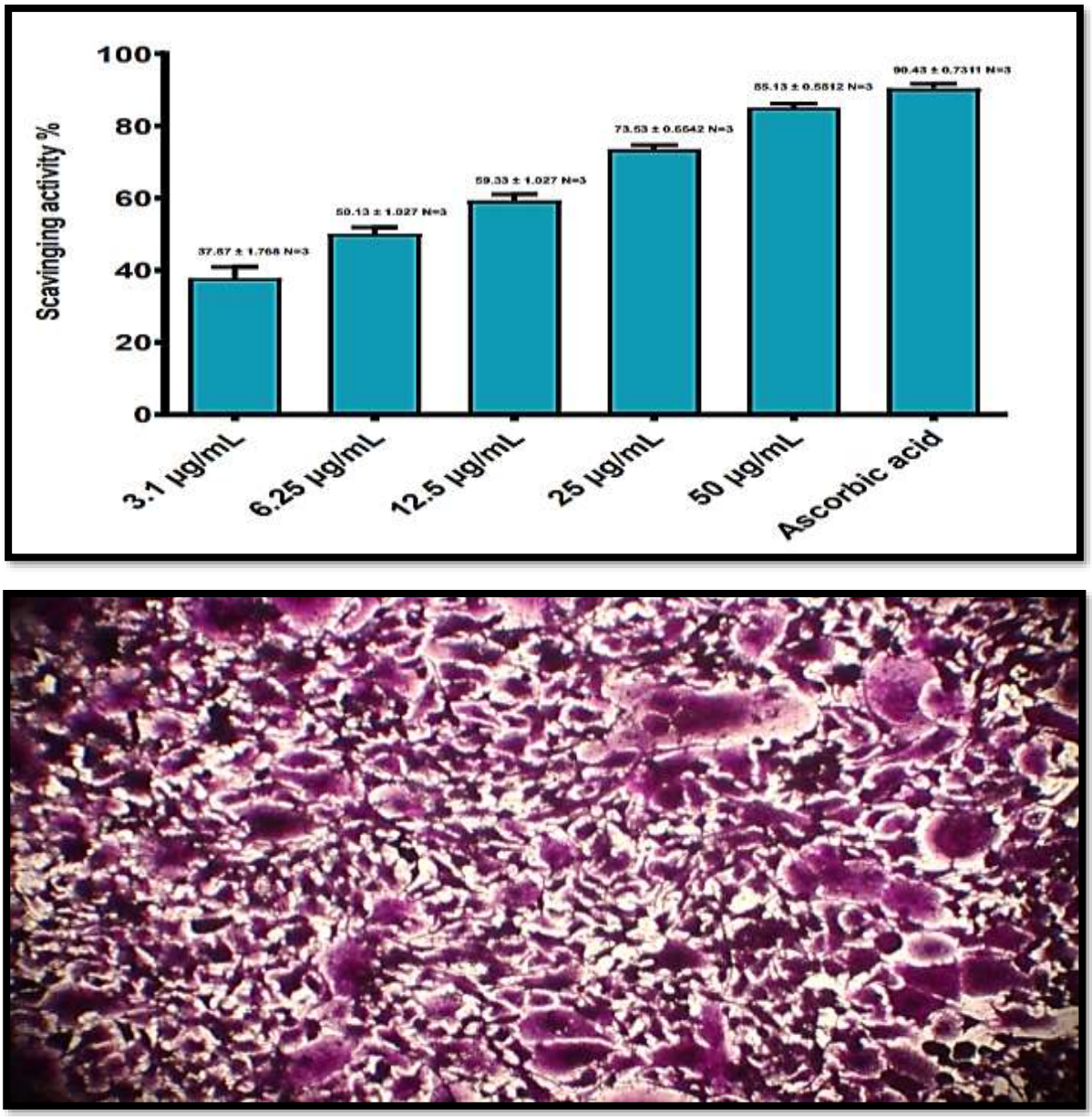

Figure 17. Antioxidant activity of Ab-AuNPs, Ascorbic acid (10µg/ml) as a positive control. The results are represented as the mean ± SD.

4.Discussion

This study biosynthesized Ab-AuNPs for the first time, using the gold solution and *A. baumannii* broth culture. Bacterial broth culture contains polysaccharides, amino acids, peptides, proteins, and enzymes. Ab-AuNPs were synthesized when the broth culture changed color from pale yellow to deep purple. These compounds can act as capping and reducing agents. These findings support previous research that showed metal biotransformation might involve capping proteins orpeptides and reductases, quinines, cytochromes, or electron shuttles to decrease metals and metal oxides [18, 19].

This study added a fixed volume of gold solution to many broth cultures. As the broth culture volume increased, the color shift rose, indicating that AuNPs had more reducing and capping agents.

The UV-Visible spectra of AuNPs within the visible absorbance band agree with [20]. Ab-AuNPs had SPR bands at 574 nm in their UV-Visible spectra (500 nm-600 nm). FTIR analysis of A. baumannii broth culture-produced Ab-AuNPs revealed the solution-stabilizing biomolecules. *A. baumannii* broth culture AuNPs produced strong bands at (3321.42, 2823.79, 2144.84, and 1631.78) cm^{-1}. These bands are amide III, polypeptides, and proteins [21]. *A. baumannii* broth culture polypeptides capped AuNPs. Strong peaks at (578.64-748.38) cm^{-1}indicate AuNP vibration. AuNPs were created [22]. The XRD spectrum has four major peaks, according to Bragg's reflection of AuNPs described in a prior work using external and intracellular culture supernatants of bacteria and yeast [23]. The primary peaks at 111, 200, 220, and 311 match reflections with Bragg angles 38.18°, 44.51°, 64.80°, and 77.72°. These results indicate high-purity AuNPs. The Debye-Scherrer equation estimates Ab-AuNPs' average crystallite size at 26.82 nm. Our results match yeast-produced AuNPs, bacteria [30], and plant extracts [24]. According to Transmission Electron Microscope (TEM) analysis, AuNPs biosynthesized using the *A. baumannii* broth culture ranged from (20-90) nm to 66 nm. Grouped and semi-spherical. These findings match previous research. [27]. The shape and size of the AuNPs biosynthesized using the *A. baumannii* broth culture are similar to the transmission electron microscopy findings, according to the field emission scanning electron microscopy (FESEM). Bacteria broth culture constituents are principally magnesium, chloride, and potassium, sodium salts of remnants of bacterial cells, and nutrient broth. Bacteria broth culture in water dissociates the salts. It reveals the negative charge, which allows the interaction with the positive direction of gold nanoparticles. This caused accumulation, which was also observed in the examination of FESEM. Even though, the bacteria broth culture acted as a reducing agent and capping agent, the collection can still be hindered by keeping the solution at a low temperature. These findings concur with numerous researches [28].

An atomic force microscope (AFM) measures the size and shape of biosynthesized Ab-AuNPs from *A. baumannii* broth culture (AFM). 2D and 3D AFM images and AuNP size distributions are shown. Ab-AuNPs ranged in size from 15–125 nm, averaging 63.82 nm. The results match the research of Vitosha *et al*. [29]. and are close to the result you have reached in Jafarizad *et al.* [30]. In contrast, another study synthesized AuNPs of different sizes [40]. This size disparity could result from other synthesis techniques, bacteria, plant extracts, or different synthesis circumstances. And the Zeta Potential analysis showed -22 mV and values below 30 mV, showing that the particles are stable and do not aggregate. These findings concur with many studies. [31, 32]. The cytotoxicity results of Ab-AuNPs showed that proliferation was significantly increased depending on concentration; the different concentrations of Ab-AuNPs used in this study are as follows: (3.1, 6.25, 12.5,25, and 50 mg/ml). The results indicate that Ab-AuNPs are a precious source of effective anti-proliferative and cytotoxic substances. Rajan *et al.* [33] showed that MCF-7 cells treated with Ab-AuNPs were significantly reduced compared with the control cells; AuNPs killed >70 % of the cells. It is also compatible with our study. In comparison, AuNPs did not show any significant effect on MCF-10 cells, which is also in agreement with the findings of a previous study that AuNPs inhibited the proliferation of human breast cancer cells (MCF7 cell line) [34, 35]. Through changes in the shape of MCF7 cell lines, the biologically prepared gold nanoparticles were more toxic than those chemically prepared in studies with PC-3, HCT116, and HepG2 tumor cells [36]. The normal cells were the controls. MCF-10 cells showed that the treated cells kept their shape before being treated. On the other hand, MCF7 cell lines that were treated with Ab-AuNPs showed changes in their shape and permeability. [37].

DPPH radical scavenging activity matches the researcher's previous study [38]. Lifestyle changes, radiation, and pollutants disrupt the balance between antioxidant action and free radical production. Still, "Green" synthesis AuNPs have promising anticancer and antioxidant properties [39, 40].

5.Conclusion

We conclude from the present study that gold nanoparticles synthesized using *A. baumannii* broth cultures are easy to prepare, inexpensive, and non-toxic to normal cells. Meanwhile, they possess antioxidant and anticancer activity. So, it can be used as an alternative treatment.

Acknowledgements

We thank the Director of the Cell Bank of the Iraqi Center for Cancer and Medical Genetic Research. To provide us with cancerous and normal cell lines and assistance and guidance during the research completion period.

References

1. Katira, P.; Zaman, M. H.; Bonnecaze, R.T. How changes in cell mechanical properties induce cancerous behavior. *Physical Review Letters*, **2021**; *108*, 2, 028103.

2. Bai Aswathanarayan, J.; Rai Vittal, R.; Muddegowda, U. Anticancer activity of metal nanoparticles and their peptide conjugates against human colon anorectal carcinoma cells. *Artificial Cells, Nanomedicine, and Biotechnology*, **2018**; *46*, 7, 1444-1451.

3. Sieja, K.; Talerczyk, M. Selenium is an element in treating ovarian cancer in women receiving chemotherapy. *Gynecologic Oncology*, **2004**; *93*, 2, 320-327.

4. Elmore, J.G.; Armstrong, K.; Lehman, C.D.; Fletcher, S.W. Screening for breast cancer. *Jama*, **2005**; 293, 10, 1245-1256.

5. Lerman, C.; Lustbader, E.; Rimer, B.; Daly, M.; Miller, S.; Sands, C.; Balshem, A. Effects of individualized breast cancer risk counseling: a randomized trial. *JNCI: Journal of the National Cancer Institute*, **1995;** *87*, 4, 286-292.

6. Khan, A.K.; Rashid, R.; Murtaza, G.; Zahra, A.J.T.R. Gold nanoparticles: synthesis and applications in drug delivery. *Tropical journal of Pharmaceutical Research*, **2014**; *13*, 7, 1169-1177.

7. Jadoun, S.; Chauhan, N.; Zarrintaj, P. Synthesis of nanoparticles using microorganisms and their applications: A review. *Environmental Chemistry Letters*, **2022**; 1-45.

8. Buzea, C.; Pacheco, I.I.; Robbie, K. Nanomaterials and nanoparticles: sources and toxicity. *Biointerphases*, **2007**; *2*, 4, MR17-MR71.

9. Heidary, M.; Nasiri, M.J.; Dabiri, H.; Takashi, S. Prevalence of drug-resistant Klebsiella pneumoniae in Iran: a review article. *Iranian Journal of Public Health*, **2018**; *47*, 3, 317.

10. Sabir, S.; Zahoor, M.A.; Waseem, M.; Siddique, M.H.; Shafique, M.; Imran, M.; Muzammil, S. Biosynthesis of ZnO nanoparticles using bacillus subtilis: characterization and nutritive significance for promoting plant growth in *Zea mays* L. *Dose-Response*, **2020**; *18*, 3, 1559325820958911.

11. Ali, I.H.; Jabir, M.S.; Al-Shmgani, H.S.; Sulaiman, G.M.; Sadoon, A.H. Pathological and immunological study on infection with escherichia coli in ale balb/c mice. *Journal of Physics: Conference Series*, **2018**; *1003*, 1, 012009.

12. Khashan, K.S.; Badr, B.A.; Sulaiman, G.M.; Jabir, M.S.; Hussain, S.A. Antibacterial activity of Zinc Oxide nanostructured materials synthesis by laser ablation method. *Journal of Physics: Conference Series*, **2021**; *1795*, 1, 012040),

13. Al Salman, H.N.K.; Ali, E.T.; Jabir, M.; Sulaiman, G.M.; Al Jadaan, S.A. 2 Benzhydrylsulfinyl N hydroxycarbamide Na extracted from fig as a novel cytotoxic and apoptosis inducer in SKOV 3 and AMJ 13 cell lines via P53 and caspase 8 pathway. *European Food Research and Technology*, **2020**.

14. Jabir, M.; Sahib, U.I.; Taqi, Z.; Taha, A.; Sulaiman, G.; Albukhaty, S.; Rizwana, H. Linalool-loaded glutathione-modified gold nanoparticles conjugated with CALNN peptide as apoptosis inducer and NF-κB translocation inhibitor in SKOV-3 cell line. International Journal of Nanomedicine, **2020;** *15*, 9025.

15. Younus, A.; Al-Ahmer, S.; Jabir, M. Evaluation of some immunological markers in children with bacterial meningitis caused by Streptococcus pneumonia. *Research Journal of Biotechnology*, **2019**; *14*, 131-133.

16. Ismail, E.H.; Saqer, A.M.; Assirey, E.; Naqvi, A.; Okasha, R.M. Successful green synthesis of gold nanoparticles using a Corchorus olitorius extract and their antiproliferative effect in cancer cells. *International Journal of Molecular Sciences*, **2018**; *19*, 9, 2612.

17. Langford, J.I.; Wilson, A.J.C. Scherrer after sixty years: a survey and new results in determining crystallite size. *Journal of Applied Crystallography*, **1978**; *11*, 2, 102-113.

18. Al-Kalifawi, E.J. Silver Nanoparticles Synthesis by Hamza's Khubdat (AS)(Kombucha) Tea and used in Burn Wounds Treatment. *J. Glob. Pharma Technol.*, **2018**; *10*, 489.

19. Hawar, S.N. Extracellular Enzyme of Endophytic Fungi Isolated from Ziziphus spina Leaves as Medicinal Plant. *International Journal of Biomaterials*, **2022**.

20. Swami, A.; Mittal, S.; Chopra, A.; Sharma, R.K.; Wangoo, N. Synthesis and pH-dependent assembly of isotropic and anisotropic gold nanoparticles functionalized with hydroxyl-bearing amino acids. *Applied Nanoscience*, **2018;** *8*, 3, 467-473.

21. Santhoshkumar, J.; Rajeshkumar, S., Kumar, S.V. Phyto-assisted synthesis, characterization, and applications of gold nanoparticles–A review. *Biochemistry and Biophysics Reports*, **2017;** *11*, 46-57.

22. Swami, A.; Mittal, S.; Chopra, A., Sharma, R.K.; Wangoo, N. Synthesis and pH-dependent assembly of isotropic and anisotropic gold nanoparticles functionalized with hydroxyl-bearing amino acids. *Applied Nanoscience*, **2018;** *8*, 3, 467-473.

23. Akintelu, S.A.; Olugbeko, S.C.; Folorunso, A.S. A review of synthesis, optimization, characterization, and antibacterial application of gold nanoparticles synthesized from plants. *International Nano Letters*, **2020**; *10*, 4, 237-248.

24. Singaravelu, G; Arockiamary, J.S.; Kumar, V.G.; Govindaraju, K. A novel extracellular synthesis of monodisperse gold nanoparticles using marine alga, Sargassum wightii Greville. *Colloids and surfaces B: Biointerfaces*, **2007**; *57*, 1, 97-101.

25. Song, J.Y.; Jang, H.K.; Kim, B.S. Biological synthesis of gold nanoparticles using Magnolia kobus and Diospyros kaki leaf extracts. *Process Biochemistry*, **2009**; *44*, 10, 1133-1138.

26. Zhang, X.; Qu, Y.; Shen, W.; Wang, J.; Li, H., Zhang, Z.; Zhou, J. Biogenic synthesis of gold nanoparticles by yeast Magnusiomyces ingens LH-F1 for catalytic reduction of nitrophenols. *Colloids and Surfaces A: Physicochemical and Engineering Aspects*, **2016**; *497*, 280-285.

27. Sharma, N.; Pinnaka, A.K.; Raje, M.; Fnu, A.; Bhattacharyya, M.S.; Choudhury, A.R. The exploitation of marine bacteria for the production of gold nanoparticles. *Microbial Cell Factories*, **2012**; 11, 1, 1-6.

28. Luzala, M.M.; Muanga, C.K.; Kyana, J.; Safari, J.B.; Zola, E.N.; Mbusa, G.V.; Memvanga, P.B. A Critical Review of the Antimicrobial and Antibiofilm Activities of Green-Synthesized Plant-Based Metallic Nanoparticles. *Nanomaterials*, **2022**; *12*, 11, 1841.

29. Vitosha, M.; Palanisamy, S.; Muthukrishnan, R.; Selvam, S.; Kannapiran, E.; You, S.; Prabhu, N.M. Biogenic synthesis of gold nanoparticles from Halymenia dilatata for pharmaceutical applications: Antioxidant, anticancer, and antibacterial activities. *Process Biochemistry*, **2019**; *85*, 219-229.

30. Jafarizad, A.; Safaee, K.; Gharibian, S.; Omidi, Y.; Ekinci, D. Biosynthesis and in-vitro study of gold nanoparticles using Mentha and Pelargonium extracts. *Procedia Materials Science*, **2015**; *11*, 224-230.

31. Owaid, M.N.; Al-Saeedi, S.S.S.; Abed, I.A. Biosynthesis of gold nanoparticles using yellow oyster mushroom Pleurotus cornucopiae var. citrinopileatus. *Environmental Nanotechnology, Monitoring & Management*, **2017**; *8*, 157-162.

32. Aljabali, A.A.; Akkam, Y.; Al Zoubi, M.S.; Al-Batayneh, K.M.; Al-Trad, B.; Abo Alrob, O.; Evans, D.J. Synthesis of gold nanoparticles using leaf extract of Ziziphus zizyphus and their antimicrobial activity. *Nanomaterials*, **2018**; *8*, 3, 174.

33. Naser, D.K.; Abbas, A.K.; Aadim, K.A. Zeta potential of Ag, Cu, ZnO, CdO, and Sn nanoparticles prepared by pulsed laser ablation in a liquid environment. *Iraqi Journal of Science*, **2020**; 2570-2581.

34. Maeh, R.K.; Jaaffar, A.I.; Al-Azawi, K.F. Preparation of Juniperus extract and detection of its antimicrobial and antioxidant activity. *The Iraqi Journal of Agricultural Science*, **2019**; *50*, 3, 1153-1161.

35. Oh Abdullah, A.M. Green synthesis of aunps from the leaf extract of Prosopis fractal for antibacterial and anti-cancer applications. *Digest Journal of Nanomaterials and Biostructures*, **2020**; *15*, 3, 943-951.

36. Yas, R. M., Ghafoor, A.; Saeed, M.A. Anticancer effect of green synthesized gold nanoparticles using orchid extract and their characterizations on breast cancer AMJ-13 Cell line. *Syst. Rev. Pharm*, **2021**; *12*, 500-505.

37. Hosny, M.; Fawzy, M.; Abdelfatah, A.M.; Fawzy, E.E.; Eltaweil, A.S. Comparative study on the potentialities of two halophytic species in the green synthesis of gold nanoparticles and their anticancer, antioxidant, and catalytic efficiencies. *Advanced Powder Technology*, **2021**; *32*, 9, 3220-3233.

38. El Domany, E.B.; Essam, T.M.; Ahmed, A.E.; Farghali, A.A. Biosynthesis Physico-chemical optimization of gold nanoparticles as anti-cancer and synergetic antimicrobial activity using Pleurotus ostreatus fungus. *Journal of Applied Pharmaceutical Science*, **2018**; *8*, 5, 119-128.

39. Razzaq, H.; Saira, F.; Yaqub, A.; Qureshi, R.; Mumtaz, M.; Saleemi, S. Interaction of gold nanoparticles with free radicals and their role in enhancing the scavenging activity of ascorbic acid. *Journal of Photochemistry and Photobiology B: Biology*, **2016**; *161*, 266-272.

40. Desai, M.P.; Sangaokar, G.M.; Pawar, K.D. Kokum fruit-mediated biogenic gold nanoparticles with photoluminescent, photocatalytic, and antioxidant activities. *Process Biochemistry*, **2018**; *70*, 188-197.